Differential Evolution Techniques for the Structure-Control Design of a Five-Bar Parallel Robot

Miguel G. Villarreal-Cervantes[a*] , Carlos A. Cruz-Villar[a], Jaime Alvarez-Gallegos[a] and Edgar A. Portilla-Flores[b]

[a]*Cinvestav-IPN, Departamento de Ingeniería Eléctrica, Av. IPN 2508, Apdo. Postal 14-740, 07300 México D.F., México*; [b]*CIDETEC-IPN, Departamento de Posgrado, Area de Mecatrónica, Av. Juán de Dios Bátiz s/n Esq. Miguel Othon de Mendizabal, Unidad Profesional Adólfo López Mateos, 07700, México D.F., México*

(*Received 00 Month 200x; final version received 00 Month 200x*)

The present work deals with the use of a constraint-handling differential evolution (CHDE) algorithm to solve a nonlinear dynamic optimization problem (NLDOP) with fifty one decision variables. A novel mechatronic design approach is proposed as a NLDOP, where both the structural parameters of a nonredundant parallel robot and the control parameters are simultaneously designed with respect to a performance criterion. Besides, the dynamic model of the parallel robot is included into the NLDOP as an equality constraint. The obtained solution will be a set of optimal geometric parameters and optimal PID control gains. The optimal geometric parameters adjust the dynamic and the kinematic parameters, optimizing then, the link shapes of the robot. The proposed mechatronic design approach is applied to simultaneously design both the mechanical structure of a five-bar parallel robot and the PID controller.

Keywords: Differential evolution; parallel robot; integrated design; dynamic optimization problem

1. Introduction

Optimization problems are frequently found in engineering applications. One of the most common approaches to formulate a parametric design problem is to consider it as an optimization problem. The integration of mechanical and electronic elements in mechatronic systems has originated a multidisciplinary framework for their design (Youcef-Toumi

*Corresponding author. Email: gvillarr@cinvestav.mx

1996). In this multidisciplinary design approach a whole description of the system behavior is needed, where the mechanical behavior and the dynamic performance must be considered. Some works in mechatronic system design propose an integrated design approach in order to fulfill the multidisciplinary framework (Portilla-Flores *et al.* 2007, Alvarez-Gallegos *et al.* 2005, Cruz-Villar *et al.* 2009). Hence, the integrated design approach is stated as a NLDOP in order to obtain a set of dynamic and kinematic parameters of the system. In most of the cases, the NLDOP implicates a set of criteria to satisfy in order to measure the system performance, such that a multiobjective optimization problem (MOP) is formulated. A typical method to handle MOPs consists of transforming the original problem into a weighted sum approach (Osyczka 1984). This transformation will be easier to solve than the original multiobjective problem.

Several mathematical programming methods such as sequential quadratic programming (SQP) are used to solve a NLDOP. However, a weakness of these methods is that they can be attracted by local minima in the neighborhood of the starting point. Moreover, these methods are able to produce only one possible solution. In order to save this problem, various points are needed to initialize the solution search, nevertheless a considerable sensitivity to its initial search point is observed on the algorithm convergence (Cruz-Villar *et al.* 2009). Also, these methods involves computing the gradient and the Hessian of the objective function and constraints, which implies that the continuity of the second order must be ensured (Portilla-Flores *et al.* 2007).

Hence, stochastic methods such as evolutionary algorithm (EAs), genetic algorithms (GA) or particle swarm optimization (PSO) can be used in order to overcome the above drawbacks. That is, the development of efficient optimization algorithms remains as an active research area. Some advantages are obtained when stochastic methods are used to solve this kind of optimization problem: 1) These methods are population-based methods. Therefore a global minima solution can be reached, although not in all kind of problems. 2) In order to start the search, additional information is not necessary; that is: gradients, Hessian matrix, initial search point, etc. 3) With these methods, complex problems can be solved. Which means, the optimization problem can include discontinuous physical models. 4) Finally, these methods are independent of the problems characteristics. That is, these methods can be used and/or adapted to a large set of problems.

Several extensions of the EAs and PSO have been suggested during the last decades offering improved performance on selected benchmark problems. Recently, another search heuristic called differential evolution (DE) has shown superior performance than PSO and EAs in the widely used benchmark problems as it is observed in (Vesterstrom and Thomsen 2004). DE is robust, that is, it is able to reproduce the similar results consistently over many trials, whereas the performance of PSO is more dependent on the randomized initialization of the individuals. As a result, PSO must be executed several times to ensure good results, whereas one run of DE is usually sufficient. Therefore, the DE algorithm is used in this paper.

Differential evolution (DE) is a population-based evolutionary algorithm (Price *et al.* 2005) with a special recombination operator that performs a linear combination of a number of individuals (normally three) and one parent (which is subject to be replaced) to create one child. The selection is deterministic between the parent and the child (the best of them remain in the next population). Moreover, the DE algorithm is easy to implement due to design variables are encoded as floating point variables and few control parameters are required. The DE algorithm can efficiently find the neighborhood of the global optimum. DE has been successfully applied to optimize mechanical systems (Portilla-Flores *et al.* 2007, Alvarez-Gallegos *et al.* 2005, Cruz-Villar *et al.* 2009, Deb and

Kain 2003, Shiakolas *et al.* 2005).

It is important to remark that only few works use DE to tackle the mechatronic design problem as a NLDOP (Portilla-Flores *et al.* 2007, Alvarez-Gallegos *et al.* 2005, Saravanan and Ramabalan 2008). A concurrent design methodology to formulate the mechatronic design problem is proposed in (Portilla-Flores *et al.* 2007) and (Alvarez-Gallegos *et al.* 2005). In such methodology the mechatronic design problem is stated as a dynamic optimization problem. A concurrent design of a pinion-rack continuously variable transmission (CVT) is carried out. It means that both the parametrical optimal design and the proportional and integral (PI) controller gains of a CVT are obtained. Both the kinematic and the dynamic models of the mechanical structure, and the dynamic of the controller are considered together as well as two system performance criteria. The resulting problem is solved using two methods: a mathematical programming method and an heuristic approach. In (Saravanan and Ramabalan 2008) a general method for computing minimum cost trajectory planning for industrial robot manipulators is presented. The aim is the minimization of a cost function with constraints namely joint positions, velocities, jerks and torques by considering dynamic equations of motion. A clamped cubic spline curve is used to represent the trajectory and a non-linear constrained optimization problem is presented. The cost function is a weighted balance of transfer time, mean average of actuators efforts and power, singularity avoidance, joint jerks and joint accelerations.

Traditionally, serial robotic systems (Lung-Wen 1999) have been used in factories for high-precision routine operations. Nonetheless, parallel robots, which consist of one or more closed kinematic chains, have been recently used due to their advantages in comparison with the serial robots. Those advantages involves high stiffness, speed and acceleration, good dynamic characteristics and precise positioning capability (Hunt 1983). However, the main disadvantages are more singularity configurations and the lack of well developed tools for analysis, synthesis, control and trajectory planning. Hence, the parallel robot design is a huge challenge because it is not an easy task to find the mechanical and the control parameters that improve the system performance.

Several design methodologies to parallel robots have been proposed. A sequential and iterative process is one of the most used methodologies to design parallel robots. That methodology is usually composed of two design phases: the mechanical design which the structural design variables are determined; followed by the control system design where the dynamic behavior is considered. Nevertheless, the robot performance depends on the simultaneous interaction between both design (Youcef-Toumi 1996). On the other hand, a design approach for a five-bar parallel robot and nonlinear PD controller gains is stated for the trajectory tracking problem in (Ouyang *et al.* 2003). The key idea of this approach is to find the dynamic (masses, mass center lengths, mass center angles, inertias) and kinematic (link lengths) parameters of the links that produce the best mass distribution in the parallel robot. The main idea of finding the best mass distribution is to simplify the dynamic model. Once the dynamic and the kinematic parameters are found, the control strategy is designed. But that results in a lack of integration in the design, that typically requires several redesigns to achieve an aceptable system performance.

Another way to state the parallel robot design for the tracking of few points in the Cartesian space is proposed in (Affi *et al.* 2007). In that work, authors take into account the Cartesian positioning error, the maximum current variation and the current fluctuation to be optimized in order to find dynamic and kinematic parameters of a four-bar parallel robot. In order to simplify the control strategy and minimize the power consumption of the motor, the velocity of the crank is set as a constant. That means

the dynamic model (dynamic behavior) is not considered in the optimization process. So, the optimization problem is an approximation of the real design problem and this problem results in a static one. A static optimization problem (Betts 2001) results when the behavior of the performance function does not depend on the time. Hence in the optimization problem, the time variable is not included and/or the system dynamics is not considered. The system dynamics is a function where the time variable is considered and this dynamics is represented by nonlinear differential equations (NLDEs) and described by a set of dynamic variables referred as the state equations. The NLDEs describe the dynamic behavior of the system, such as mass and energy balances, and algebraic equations that ensure physical and electrical relations.

On the other hand, singularity configurations are some of the most significant and critical problems in the design and control of parallel robots. Unlike serial robots, operation of parallel robots near a singular point can cause severe destruction of the robot. Several papers (Klein and Blaho 1987, Yoshikawa 1990, Kim 2006) have established performance indexes derived from the Jacobian matrix in order to avoid singularities. Optimal robot configurations (optimal position) and optimal link lengths are found with those indexes. In (Kim 2006), a kinematic design (static optimization problem) based on the tracking task of a few Cartesian points for a parallelogram five-bar parallel robot is proposed. In that work, the optimal link lengths are only found in one single design step without considering the control parameters.

In (Ouyang *et al.* 2003, Affi *et al.* 2007, Kim 2006), the optimal dynamic and kinematic parameters of the links do not give to the designer an idea of the link shapes, therefore other optimization process will be required for the optimal geometric design of the links. In addition, in order to compute the inertias of the links, the link shapes must be known. Nevertheless in those works the following assumption is considered: the inertias were computed as if the links were cylindrical or rectangular geometries due to the unknown shapes of links. Also, a static optimization problem is stated since the system dynamics is not taken into consideration as an equality dynamic constraint (Betts 2001). As a result, the found optimal design does not provide the best performance in the real word due to the lack of system dynamics into the optimization problem and due to the above assumption.

The main contributions of the present work is to state a mechatronic design as a nonlinear dynamic optimization problem. The mechatronic design must consider the synergy between the mechanical design of a non redundant parallel robot and the control design. The target of the mechatronic design is to simultaneously find the optimum structure-control parameters so that the end-effector of the parallel robot can track a desired trajectory without singularity configurations. In addition, this work deals with the use of a constraint-handling differential evolution (CHDE) algorithm (Mezura-Montes *et al.* 2004) to solve such nonlinear dynamic optimization problem where nonlinear differential equations are included as constraints. A modification of this algorithm is included for saving time in the evaluation of the performance function. The obtained solution will be a set of optimal geometric parameters and optimal PID control gains. The optimal geometric parameters adjust the dynamic and kinematic parameters and the link shapes of the robot such that, other optimization process is not required to adjust the geometry of the robot links (link shapes). The mechatronic design is efficiently applied to the mechanical design of the five-bar parallel robot and the PID control design.

This paper is organized as follows: the five-bar parallel robot with its controller is presented in Section 2. The formulation of the mechatronic design approach is stated in Section 3, where each part of the dynamic optimization problem for the particular

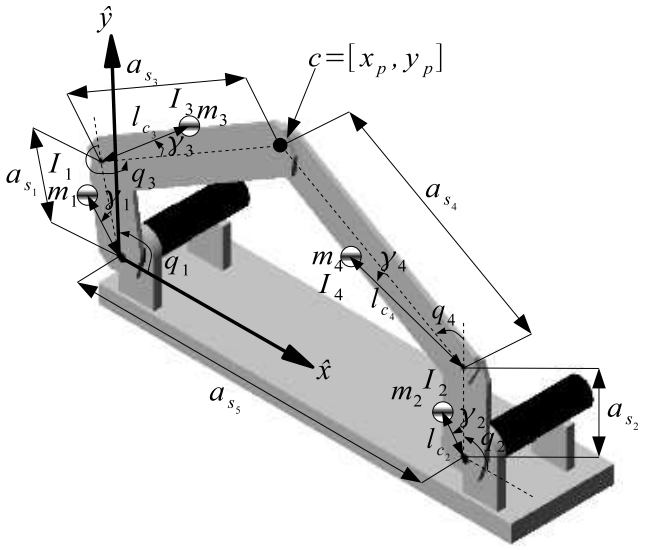

Figure 1. Schematic diagram of the five-bar parallel robot.

case of the five-bar parallel robot design and its control design is detailed. In Section 4, the evolutionary algorithm is presented. The results and discussion of the dynamic optimization problem are carried out in Section 5, where the results and discussions of the optimal structure-control design parameters for the five-bar parallel robot are presented too. Finally, conclusions of this approach are presented in Section 6.

2. Five-bar parallel robot

The five bar parallel robot is a non redundant robot consisting of five revolute joints with two of them active (Fig. 1). The reduced model method of closed chain mechanisms presented in (Ghorbel *et al.* 2000) is employed to obtain the dynamic model of the five-bar parallel robot. The dynamic parameters of the $i-th$ link are the mass m_i, the distance of the mass center l_{c_i}, the inertia I_i and the angle of the mass center γ_i. The kinematic parameter is the link length a_{s_i}. In Fig. 1 these parameters are shown.

The dynamic model of the five-bar parallel robot is shown in (1), where $q = [q_1, q_2]^T \in R^2$, $\dot{q} = [\dot{q}_1, \dot{q}_2]^T \in R^2$ are independent generalized coordinate vectors of position and velocity of the actuated links respectively. $q' = [q_1, q_2, q_3, q_4]^T \in R^4$, $\dot{q}' = [\dot{q}_1, \dot{q}_2, \dot{q}_3, \dot{q}_4]^T \in R^4$ are dependent coordinate vectors of position and velocity. q_3 and q_4 are the angular positions of unactuated links and $u = [u_1, u_2]^T \in R^2$ is the applied generalized force vector. $D(q') = \rho(q')^T D'(q')\rho(q') \in R^{2\times 2}$ is a symmetric positive definite inertia matrix, $C(q', \dot{q}') = \rho(q')^T C'(q', \dot{q}')\rho(q') + \rho(q')^T D'(q')\dot{\rho}(q') \in R^{2\times 2}$ is the Coriolis and centrifugal matrix, $g(q') = \rho(q')^T g'(q') \in R^2$ is the gravity vector, $\bar{c} = [\bar{x}_p, \bar{y}_p]^T$ and $\dot{\bar{c}} = [\dot{\bar{x}}_p, \dot{\bar{y}}_p]^T$ are the position and velocity in the Cartesian space of the desired trajectory to be executed by the end-effector of the robot. $\sigma(q)$ involves a parameterization of $q \to q'$, $\rho(q') = \left[\frac{\partial\sigma(q)}{\partial q}, \frac{\partial\sigma(q)}{\partial q'}\right] \in R^{4\times 2}$, $\dot{\rho}(q') = \frac{d(\rho(q'))}{dt} \in R^{4\times 2}$ and $D'(q') \in R^{4\times 4}$, $C'(q') \in R^{4\times 4}$, $g'(q') \in R^4$ are motion equations of two serial robots when the parallel robot is virtually

cut open at the end-effector (Ghorbel *et al.* 2000).

$$\begin{aligned} \ddot{q} &= D^{-1}(q')\left(-C(q',\dot{q}')\dot{q} - g(q') + u\right) \\ \dot{q}' &= \rho\left(q'\right)\dot{q} \\ q' &= \sigma\left(q\right) \end{aligned} \tag{1}$$

The main characteristic of the parallel robot dynamic model that makes the difference to serial robot models (Spong and Vidyasagar 2004), is that there exist more singularity configurations in the workspace and it is defined on a compact set where closed-chain constraints are satisfied and singularity configurations are avoided. A manipulator is said to be at a singularity configuration when the Jacobian matrix losses its full rank (Lung-Wen 1999). Therefore, at a singularity configuration, a manipulator may lose one or more degrees of freedom, and it will not be able to follow some trajectories in the end-effector space. It follows that all control laws for open chain robots could also be applied with the only restriction that the guaranteed (Lyapunov) stability conclusions will be local (Ghorbel *et al.* 2000). In addition, some parallel robot dynamic models have implicit equations requiring a numerical method to solve. For the particular case of the five-bar parallel robot, the dynamic model is an explicit equation.

2.1. *Control system*

In the last decades, researchers have been developing new and sophisticated control laws in order to improve the system performance from the control system standpoint. Nevertheless, in most of the cases the control system calibration is quite difficult requiring previous experience to tune the control system.

On the other hand, from the mechatronic design standpoint (Li *et al.* 2001), the performance of a robot relies on both the control system design and the mechanical system design. The mechatronic design does not focus on developing neither new control strategies nor a new mechanical system. The idea of a mechatronic design is to find a compromise between the control system design and the mechanical system design in order to improve the mechatronic system performance, considering control laws easy to implement and a predefined robot structure. Therefore, based on the idea of a mechatronic design, two PID controllers are chosen, since the PID controller has an appropriate performance in most of the applications and it is widely accepted by several industrial control processes despite of the development of many others control strategies. Therefore with the PID controller, the input vector $u = [u_1, u_2]^T$ is defined in (2).

$$u_i = k_{p_i} e_i + k_{i_i} \int_0^{t_f} e_i dt + k_{d_i} \dot{e}_i \qquad \text{for } i = 1, 2 \tag{2}$$

Due to the integrator of the PID controller, the closed loop system order is increased by one for each control input. So, the dynamic model of the five-bar parallel robot (1) with its PID controller (2) can be formulated in state variables as nonlinear differential equations (3) which must be solved by a numerical method such as Runge-Kutta method:

$$\dot{x} = \tfrac{dx}{dt} = f\left(x, \bar{x}, p, u\right) \tag{3}$$

where $x = [q_1,\ q_2,\ \dot{q}_1,\ \dot{q}_2,\ \int_0^{t_f} e_1 dt,\ \int_0^{t_f} e_2 dt]^T = [x_1, ..., x_6]^T \in R^6$ and $\bar{x} \in R^6$ are the current and desired state variable vectors, $e = [e_1, e_2]^T = [\bar{x}_1 - x_1, \bar{x}_2 - x_2]^T$ and $\dot{e} = [\dot{e}_1, \dot{e}_2]^T = [\bar{x}_3 - x_3, \bar{x}_4 - x_4]^T$ are the angular position and velocity error vectors of the actuated angles, respectively, t is the time, $t_f \in R$ is the final time and $p \in R^{n_p}$ is a vector of all design variables where the mechanical and controller parameters of the system are included.

3. Structure-Control Integrated design approach

Dynamic optimization is the process of determining control and state histories for a dynamic system over a finite time period to minimize a performance index (BrysonJr. 1999). That is, an optimal control problem (OCP) for a dynamic continuous system consist in finding the time history of a control vector $u(t)$ for $t_0 < t < t_f$ to minimize a performance index of the form:

$$J = \Phi[x(t_f)] + \int_{t_0}^{t_f} L(x(t), u(t), p, t) dt \tag{4}$$

subject to:

$$\begin{aligned} \frac{dx}{dt} &= f(x(t), u(t), p, t) \\ x(t_0) &= x_0 \end{aligned} \tag{5}$$

with t_0, t_f and x_0 specified.

In the general optimal problem, an n-dimensional state vector stated by $x(t)$ describes the behavior of the system at time t. Also, an m-dimensional control vector $u(t)$ determines the time rate of change of the state vector through the set of Ordinary Differential Equations (ODE's) stated by (5). p is the time-independent parameter vector.

Dynamic optimization problems can be solved either by variational approaches or by applying some level of discretization that converts the original continuous time problem into a discrete time problem (Kameswaran and Biegler 2006). The variational approaches are focused on obtaining a solution to the classical necessary conditions for optimality (BrysonJr. 1999). These approaches are also known as indirect methods. The second approaches are the methods that discretize the original continuous time formulation can be divided into two categories, according to the level of discretization. The first category consists of methods that discretize only the control profiles (partial dicretization methods) and the second one consists of the methods that discretize the state and control profiles (full discretization methods). The partially discretized problem can be solved either by dynamic programming or by applying a nonlinear programming (NLP) strategy and they are known as control parametrization methods (Betts 2001). A basic characteristic of these approaches is that every iteration a feasible solution of the ODE's system, for given control values, is obtained by integration. The main advantage of these approaches is that they generate smaller discrete problems than full discretization methods. The full discretization problem can only be solved by NLP but the basic characteristic is that they solve the ODE's only once, at the optimum. The full discretization method is larger and may require special solution techniques (Kameswaran and Biegler 2006).

In order to solve the OCP, a control parametrization method can be used. The idea is to transform the infinite dimensional OCP into a finite dimensional optimization problem or NLP problem, where the trajectory generation (state vector $x(t)$) and the feedback design of a control system (control vector $u(t)$) can be considered as two separate problems. That is, the design of a control system can be computed based on a control vector parameterization (CVP) while the trajectory generation is subject to fulfill the set of ODEs stated by (5). The control parameterization method is used in several works as in Cruz-Villar *et al.* (2009) and Sadegh and Driessen (1999). Therefore, in this work the control vector is parameterized using PID controllers. This control vector parameterization is stated in (2). Without loss of generality in the integrated design framework, the problem stated in (4)-(5) is rewritten as:

$$\begin{aligned} \underset{p}{Min} \quad & \bar{J}(x, \bar{x}, \bar{c}, \dot{\bar{c}}, p, t) \\ & \bar{J} = \int_{t_0}^{t_f} L(x, \bar{x}, \bar{c}, \dot{\bar{c}}, p, t) dt \end{aligned} \tag{6}$$

subject to:

$$\frac{dx}{dt} = f\left(x, \bar{x}, p, t\right), x(t_0) = x_0 \tag{7}$$

$$g_j(x, \bar{x}, \bar{c}, \dot{\bar{c}}, p, t) < 0, \text{ for } j = 1, \ldots, n_g \tag{8}$$

$$h_k(x, \bar{x}, \bar{c}, \dot{\bar{c}}, p, t) = 0, \text{ for } k = 1, \ldots, n_h \tag{9}$$

where $p \in R^{n_p}$ is a vector of all design variables involving the geometric mechanical parameters of the five-bar parallel robot and the PID controller gains, $x \in R^n$ and $\bar{x} \in R^n$ are the current and desired state variable vectors for the generalized coordinates and generalized velocities of the system dynamics, respectively, $x_0 \in R^n$ is the initial state vector required for solving the nonlinear differential equations (NLDEs) (7), $t \in R$ is the time variable, $\bar{c} \in R^{n_c}$ and $\dot{\bar{c}} \in R^{n_c}$ are the position and velocity vectors in the Cartesian space of the desired trajectory to be tracked by the system, $f\left(x, \bar{x}, p, t\right) : R^{n+n_p} \rightarrow R^n$ is a nonlinear vector function , $L(x, \bar{x}, \bar{c}, \dot{\bar{c}}, p, t) : R^{n+n_p} \rightarrow R$, $g_j(x, \bar{x}, \bar{c}, \dot{\bar{c}}, p, t) : R^{n+n_p} \rightarrow R$ and $h_k(x, \bar{x}, \bar{c}, \dot{\bar{c}}, p, t) : R^{n+n_p} \rightarrow R$ are smooth functions which correspond to the performance criterion, inequality and equality constraints referred to the system design, respectively. Then, the nonlinear dynamic optimization problem (NLDOP) for the mechatronic design of the five-bar parallel robot, is to find the design variables p that minimize (6) subject to inherent design constraints (7 - 9).

In next subsections, the performance criterion for the structure-control integrated design of the five-bar parallel robot is presented. Moreover, the design variable vector and the constraints of the NLDOP (6) - (9) are detailed.

3.1. *Performance criterion*

Singularity configuration is a typical problem in parallel robots. In a singular configuration, a manipulator may lose one or more degrees of freedom, and it will not be able to follow some trajectories in the end-effector space (Lung-Wen 1999). Hence, when it happens, the parallel robot can not be controlled.

According to the singularity classification (Liu *et al.* 2006) of the five-bar parallel robot, there are three kind of singularities: the first kind, called the stationary singularity, occurs when the end-effector reaches its workspace limit, that is, when the angles q_1 and q_3 or q_2 and q_4 are collinear (see Fig. 1). The second kind of singularity called the uncertainty singularity arises when the robot gains additional degree of freedom (d.o.f.). This kind of singularity is usually inside the workspace and it occurs when the angles q_3 and q_4 are collinear. The last kind of singularity is of a different nature than the first two, since it is not only configuration but also architecture dependent, and it occurs when all links are collinear.

A kind of distance of the robot configuration to singular ones is the manipulability measure. A large manipulability measure means singularities remoteness and a small one means singularities closeness. This measure was developed by Yoshikawa (Yoshikawa 1990) and can be applied to non redundant robots (Mayorga and Carrera 2006). As the five-bar parallel robot is a non redundant robot, the manipulability measure is a useful criterion to avoid singularity configurations. Nevertheless, the manipulability measure can not be used as the only performance criterion in a design approach where both the mechanical and control parameters (mechatronic design) are simultaneously considered, since the control objective (to follow a desired point or trajectory) could not be carried out. So, the following performance criterion (10) is proposed in order to satisfy trajectory tracking without singularity configurations.

$$\bar{J} = \int_{t_0}^{t_f} \left(\frac{e^T e}{\max_1} - \frac{2\left|\det J^{-1}\right|}{tr(J^{-1}J^{-T})} \right) dt \tag{10}$$

where:

$$J = \begin{bmatrix} -\frac{a_1(\sin(q_2+q_4))\sin q_3}{\sin(q_1-q_2+q_3-q_4)} & \frac{a_2(\sin(q_1+q_3))\sin q_4}{\sin(q_1-q_2+q_3-q_4)} \\ \frac{a_1(\cos(q_2+q_4))\sin q_3}{\sin(q_1-q_2+q_3-q_4)} & -\frac{a_2(\cos(q_1+q_3))\sin q_4}{\sin(q_1-q_2+q_3-q_4)} \end{bmatrix} \tag{11}$$

$$q_3 = \sin^{-1}\frac{a_4\sin q_4 + a_2\sin q_2 - a_1\sin q_1}{a_3}$$

$$q_4 = 2\tan^{-1}\left(\frac{-B \pm \sqrt{B^2 - 4AC_4}}{2A}\right)$$

$$A = a_4^2 + a_2^2 + a_5^2 + a_1^2 - a_3^2 + 2a_2a_5\cos(q_2) - 2a_2a_1\cos(q_2 - q_1)$$
$$-2a_5a_1\cos(-q_1) - 2a_4a_2\cos q_2 - 2a_4a_5 + 2a_4a_1\cos q_1$$

$$B = 4a_4a_2\sin q_2 - 4a_4a_1\sin q_1$$

$$C = a_4^2 + a_2^2 + a_5^2 + a_1^2 - a_3^2 + 2a_2a_5\cos(q_2) - 2a_2a_1\cos(q_2 - q_1)$$
$$-2a_5a_1\cos(-q_1) + 2a_4a_2\cos q_2 + 2a_4a_5 - 2a_4a_1\cos q_1$$

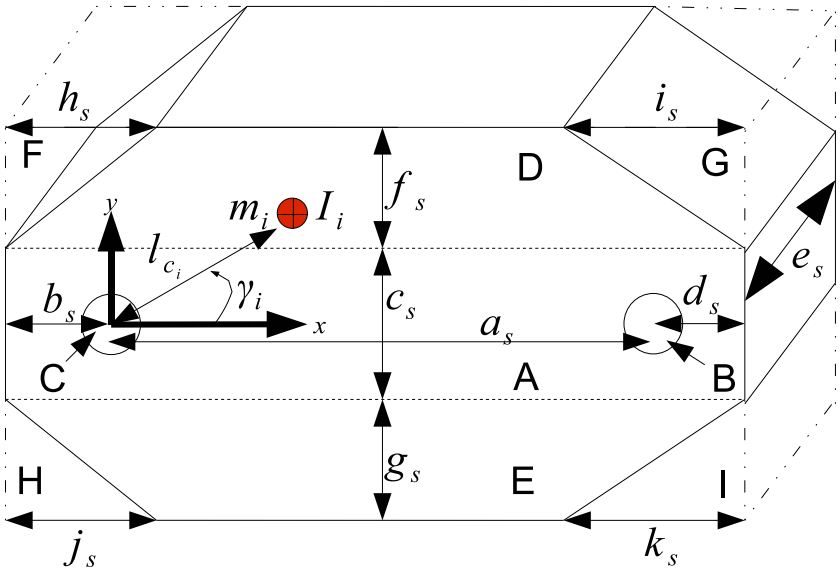

Figure 2. Schematic representation of kinematic and dynamic parameters, and the geometric parameters of the links for the five-bar parallel robot.

In (10), the first term involves the position errors where $e = [\bar{x_1} - x_1, \bar{x_2} - x_2]^T$ is the vector of angular position errors. The second term is the manipulability measure where $\det(\bullet)$ and $tr(\bullet)$ are the determinant and the trace of the matrix $(\bullet)$, and J is the Jacobian matrix of the five-bar parallel robot. $\max_1$ is the square of the maximum angular position error found in the trajectory tracking for the time interval $[0, t_f]$. So, (10) is unitless.

3.2. *Design variables*

Let us consider figure 2. In this paper an octagonal shape of the links is used because the geometric parameters of the links can modify in a wide range the dynamic parameters of the links (i. e., the mass m_i, the mass center length l_{c_i}, the mass center angle γ_i) and the kinematic parameters (i. e., link length a_{s_i}). The geometric parameters of the $i-th$ link a_{s_i}, b_{s_i}, c_{s_i}, d_{s_i}, e_{s_i}, f_{s_i}, g_{s_i}, h_{s_i}, i_{s_i}, j_{s_i}, k_{s_i}, for the five-bar parallel robot are considered as the structural design parameters to be optimized. Those parameters are selected because they can modify the dynamic and kinematic parameters of the links. Once the optimization process is finished, the optimum geometric parameters will provide the shape of the link. If those parameters are not considered and if we select only the dynamic and kinematic parameters, another optimization process would be required in order to find the structure shape.

On the other hand, the gains of the two PID controllers (k_{p_1}, k_{i_1}, k_{d_1}, k_{p_2}, k_{i_2}, k_{d_2}) are considered as the control design parameters to be optimized. So, the design parameter vector $p \in R^{51}$ which involves structural and control design parameters results as in (12):

$$p = [\, a_{s_1} \cdots a_{s_5},\, b_{s_1} \cdots b_{s_4},\, c_{s_1} \cdots c_{s_4},\, d_{s_1} \cdots d_{s_4},\, e_{s_1} \cdots e_{s_4},\, f_{s_1} \cdots f_{s_4}, \\ g_{s_1} \cdots g_{s_4},\, h_{s_1} \cdots h_{s_4},\, i_{s_1} \cdots i_{s_4},\, j_{s_1} \cdots j_{s_4},\, k_{s_1} \cdots k_{s_4} \\ k_{p_1},\, k_{p_2},\, k_{i_1},\, k_{i_2},\, k_{d_1},\, k_{d_2}\,]^T \tag{12}$$

Note in Fig 2, that the geometric parameters f_{s_i}, g_{s_i}, h_{s_i}, i_{s_i}, j_{s_i}, k_{s_i} for $i = 1$ to 4, can change the mass center angle γ_i of the $i-th$ link in a closed interval $[0, \pm\pi]$. If these parameters are not taken into account, the mass center angle of the links could be changed to the following discrete values: 0, $\pm\pi$ rad. In order to find the mathematical expression of the dynamic parameters (m_i, l_{c_i}, γ_i, I_i) of the $i-th$ link in terms of geometric parameters, it is necessary to consider the following:

- The coordinate origin is placed at the intersection of the $x-y$ axes and in the C hole as shown in Fig. 2.
- The $i-th$ link can only move at the $x-y$ plane.
- There is a shaft in the B hole at the links 1 and 3. A cylindrical support is placed on the C hole of the link 1 and two cylindrical supports are placed at the B and C holes of the link 2, respectively.
- Links and shafts are made of aluminium and steel, respectively. The density of the aluminium and the steel are $\rho_{al} = 2710\,\frac{\mathrm{Kg}}{\mathrm{m}^3}$ and $\rho_{st} = 7840\,\frac{\mathrm{Kg}}{\mathrm{m}^3}$, respectively.
- The links are divided in simple geometries in order to simplify the computing of their dynamic parameters. Therefore, the $i-th$ link is divided in nine parts A_i, B_i, C_i, D_i, E_i, F_i, G_i, H_i, I_i, as it is shown in Fig. 2.
- The $i-th$ mass is concentrated at the mass center of the $i-th$ link.

The procedure to obtain the dynamic parameters of a body is explained in (Hibbeler 2003). The dynamic parameters of the five-bar parallel robot in terms of geometric parameters are summarized in next subsections.

3.2.1. *Mass m_i*

The masses of links are shown in (13), where $m_{A_i}, ..., m_{I_i}$ are masses of the A,...,I geometric shapes, m_{xB_i} is the mass of the shaft which is placed on the B_i hole, m_{csB_i} and m_{csC_i} are masses of cylindrical supports which are placed on the B and C holes. $r_B = 3.175 \times 10^{-3}\,\mathrm{m}$ is the radius of the B hole, $r_{csB} = 15.87\,5 \times 10^{-3}\,\mathrm{m}$ and $r_{csC} = 19.05 \times 10^{-3}\,\mathrm{m}$ are radii of cylindrical supports which are placed on B and C holes respectively, $L_{cs} = 0.010\,\mathrm{m}$ is the length of the cylindrical support which is placed on C holes, and $r_i = 0.006\,\mathrm{m}$ for $i = 1, 2$ and $r_i = 0.0025\,\mathrm{m}$ for $i = 3, 4$ are radii of cylindrical supports which are placed on C hole.

$$\begin{aligned} m_1 &= m_{T_1} + m_{xB_1} + m_{csC_1} \\ m_2 &= m_{T_2} + m_{xB_2} + m_{csC_2} + m_{csB} \\ m_3 &= m_{T_3} + m_{xB_3} \\ m_4 &= m_{T_4} \end{aligned} \tag{13}$$

where:

$$
\begin{aligned}
m_{T_i} &= m_{A_i} - m_{B_i} - m_{C_i} + m_{D_i} + m_{E_i} - m_{F_i} - m_{G_i} - m_{H_i} - m_{I_i} \\
m_{xB_1} &= \rho_{st}\pi {r_B}^2 \left(e_{s_1} + e_{s_3}\right) \\
m_{xB_3} &= \rho_{st}\pi {r_B}^2 \left(e_{s_3} + e_{s_4}\right) \\
m_{csC_i} &= \rho_{al}\pi \left[{r_{csC}}^2 - {r_i}^2\right] L_{cs} \\
m_{B_i} &= \rho_{al} \left[\pi \left(r_B\right)^2 \left(e_{s_i}\right)\right] \\
m_{csB} &= \rho_{al}\pi \left[{r_{csB}}^2 - {r_B}^2\right] e_{s_3} \\
m_{C_i} &= \rho_{al} \left[\pi \left(r_i\right)^2 \left(e_{s_i}\right)\right] \\
m_{F_i} &= \frac{1}{2}\rho_{al} \left(h_{s_i}\right) \left(f_{s_i}\right) \left(e_{s_i}\right) \\
m_{G_i} &= \frac{1}{2}\rho_{al} \left(i_{s_i}\right) \left(f_{s_i}\right) \left(e_{s_i}\right) \\
m_{H_i} &= \frac{1}{2}\rho_{al} \left(j_{s_i}\right) \left(g_{s_i}\right) \left(e_{s_i}\right) \\
m_{I_i} &= \frac{1}{2}\rho_{al} \left(k_{s_i}\right) \left(g_{s_i}\right) \left(e_{s_i}\right) \\
m_{A_i} &= \rho_{al} \left[\left(a_{s_i} + b_{s_i} + d_{s_i}\right) \left(c_{s_i}\right) \left(e_{s_i}\right)\right] \\
m_{D_i} &= \rho_{al} \left[\left(a_{s_i} + b_{s_i} + d_{s_i}\right) \left(f_{s_i}\right) \left(e_{s_i}\right)\right] \\
m_{E_i} &= \rho_{al} \left[\left(a_{s_i} + b_{s_i} + d_{s_i}\right) \left(g_{s_i}\right) \left(e_{s_i}\right)\right] \\
m_{xB_2} &= \rho_{st} \left[\pi \left(r_B\right)^2 \left(e_{s_2} + e_{s_3} + e_{s_4}\right)\right]
\end{aligned}
$$

3.2.2. *Length l_{c_i} and angle γ_i of the mass center*

The mathematical expression for the length l_{c_i} and the angle γ_i of the mass center for the $i-th$ link is shown in (14). $(x_{CM_i},\ y_{CM_i})$ are the $x-y$ coordinates of the total mass center of the link, (x_{A_i}, y_{A_i}), ..., (x_{I_i}, y_{I_i}), (x_{xB_i}, y_{xB_i}), and (x_{csB}, y_{csB}) are the $x-y$ mass center coordinate for the A_i,...,I_i part, for the shaft placed on the B hole and for the cylindrical support placed on the B hole, respectively.

$$
l_{c_i} = \sqrt{\left(x_{CM_i}\right)^2 + \left(y_{CM_i}\right)^2},\ \gamma_i = A\tan 2\left(\frac{y_{CM_i}}{x_{CM_i}}\right) \tag{14}
$$

where:

$$
\begin{aligned}
x_{T_i} &= x_{A_i}m_{A_i} - x_{B_i}m_{B_i} - x_{C_i}m_{C_i} + x_{D_i}m_{D_i} + x_{E_i}m_{E_i} - x_{F_i}m_{F_i} - x_{G_i}m_{G_i} \\
&\quad -x_{H_i}m_{H_i} - x_{I_i}m_{I_i} \\
y_{T_i} &= y_{A_i}m_{A_i} - y_{B_i}m_{B_i} - y_{C_i}m_{C_i} + y_{D_i}m_{D_i} + y_{E_i}m_{E_i} - y_{F_i}m_{F_i} - y_{G_i}m_{G_i} \\
&\quad -y_{H_i}m_{H_i} - y_{I_i}m_{I_i} \\
x_{CM_1} &= \frac{x_{T_1} + x_{xB_1}m_{xB_1}}{m_1} \\
x_{CM_2} &= \frac{x_{T_2} + x_{xB_2}m_{xB_2} + x_{csB}m_{csB}}{m_2} \\
y_{H_i} &= y_{I_i} = -\left(\frac{1}{2}c_{s_i} + g_{s_i}\right) + \frac{1}{3}g_{s_i} \\
x_{xB_2} &= x_{scB_2} = a_{s_2} \\
x_{CM_3} &= \frac{x_{T_3} + (x_{xB_3})\,(m_{xB_3})}{m_3} \\
x_{CM_4} &= \frac{x_{T_4}}{m_4} \\
y_{CM_4} &= \frac{y_{T_4}}{m_4} \\
y_{F_i} &= y_{G_i} = \left(\frac{1}{2}c_{s_i} + f_{s_i}\right) - \frac{1}{2}f_{s_i} \\
y_{D_i} &= \frac{1}{2}f_{s_i} + \frac{1}{2}c_{s_i} \\
x_{D_i} &= \frac{(a_{s_i} + b_{s_i} + d_{s_i})}{2} - b_{s_i} \\
x_{E_i} &= \frac{(a_{s_i} + b_{s_i} + d_{s_i})}{2} - b_{s_i} \\
y_{CM_1} &= \frac{y_{T_1}}{m_1} \\
y_{CM_2} &= \frac{y_{T_2} + (y_{xB_2})\,(m_{xB_2}) + (y_{csB})\,(m_{csB})}{m_2} \\
y_{A_i} &= y_{B_i} = y_{C_i} = y_{xB_i} = y_{csC_i} = x_{C_i} = x_{csC_i} = 0 \\
x_{G_i} &= (a_{s_i} + d_{s_i}) - \frac{1}{3}i_{s_i} \\
x_{I_i} &= (a_{s_i} + d_{s_i}) - \frac{1}{3}k_{s_i} \\
y_{xB_2} &= y_{csC_2} = y_{csB} = y_{xB_3} = x_{csB} = x_{csC_2} = 0 \\
x_{A_i} &= \frac{(a_{s_i} + b_{s_i} + d_{s_i})}{2} - b_{s_i} \\
x_{B_i} &= a_{s_i} \\
x_{xB_3} &= a_{s_3}
\end{aligned}
$$

$$
\begin{aligned}
y_{CM_3} &= \frac{y_{T_3} + (y_{xB_3})\,(m_{xB_3})}{m_3} \\
y_{E_i} &= -\frac{1}{2}(g_{s_i} - c_{s_i}) \\
x_{F_i} &= \frac{1}{3}h_{s_i} - b_{s_i} \\
x_{H_i} &= \frac{1}{3}j_{s_i} - b_{s_i} \\
x_{xB_i} &= a_{s_i}
\end{aligned}
$$

3.2.3. *Inertia I_i*

The inertias of the links must be computed with respect to the mass center of the link, therefore the parallel axis theorem (Hibbeler 2003) is required. These inertias are computed as in (15), where $I_{A_i}, ..., I_{I_i}$ are the inertias of the A,...,I geometric shapes, respectively, I_{xB_i} is the inertia of the shaft placed at the B$_i$ hole, I_{csB} and I_{csC_2} are inertias of cylindrical supports which are placed at the B and C holes, respectively and $P_{\#}$ is an equation where the sign # represents whatever subscript, for example P_{A_i}, P_{B_i}, etc.

$$
\begin{aligned}
I_1 &= I_{T_1} + I_{xB_1} + I_{csC_1} \\
I_2 &= I_{T_2} + I_{xB_2} + I_{csC_2} + I_{csB} \\
I_3 &= I_{T_3} + I_{xB_3} \\
I_4 &= I_{T_4}
\end{aligned}
\tag{15}
$$

where:

$$
\begin{aligned}
I_{T_i} &= I_{A_i} - I_{B_i} - I_{C_i} + I_{D_i} + I_{E_i} - I_{F_i} - I_{G_i} - I_{H_i} - I_{I_i} \\
I_{I_i} &= \frac{1}{18}m_{I_i}\left[{k_{s_i}}^2 + {g_{s_i}}^2\right] + P_{I_i} \\
I_{xB_3} &= \frac{1}{2}m_{xB_3}{r_B}^2 + P_{xB_3} \\
I_{H_i} &= \frac{1}{18}m_{H_i}\left[{j_{s_i}}^2 + {g_{s_i}}^2\right] + P_{H_i}
\end{aligned}
$$

$$
\begin{aligned}
I_{xB_1} &= \frac{1}{2} m_{xB_1} {r_B}^2 + P_{xB_1} \\
I_{G_i} &= \frac{1}{18} m_{G_i} \left[{i_{s_i}}^2 + {f_{s_i}}^2 \right] + P_{G_i} \\
I_{xB_2} &= \frac{1}{2} m_{xB_2} {r_B}^2 + P_{xB_2} \\
I_{csB} &= \frac{1}{2} m_{csB} \left[{r_{csB}}^2 + {r_B}^2 \right] + P_{csB} \\
I_{B_i} &= \frac{1}{2} m_{B_i} {r_B}^2 + P_{B_i} \\
I_{F_i} &= \frac{1}{18} m_{F_i} \left[{h_{s_i}}^2 + {f_{s_i}}^2 \right] + P_{F_i} \\
I_{C_i} &= \frac{1}{2} m_{C_i} {r_i}^2 + P_{C_i} \\
I_{A_i} &= \frac{1}{12} m_{A_i} \left((a_{s_i} + b_{s_i} + d_{s_i})^2 + (c_{s_i})^2 \right) + P_{A_i} \\
I_{D_i} &= \frac{1}{12} m_{D_i} \left((a_{s_i} + b_{s_i} + d_{s_i})^2 + (f_{s_i})^2 \right) + P_{D_i} \\
I_{E_i} &= \frac{1}{12} m_{E_i} \left((a_{s_i} + b_{s_i} + d_{s_i})^2 + (g_{s_i})^2 \right) + P_{E_i} \\
P_{\#} &= m_{\#} \left(\sqrt{(x_{\#} - x_{CM_i})^2 + (y_{\#} - y_{CM_i})^2} \right)^2 \\
I_{csC_1} &= \frac{1}{2} m_{csC_1} \left[{r_{csC}}^2 + {r_i}^2 \right] + P_{csC_1} \\
I_{csC_2} &= \frac{1}{2} m_{csC_2} \left[{r_{csC}}^2 + {r_i}^2 \right] + P_{csC_2}
\end{aligned}
$$

3.3. *Constraint functions*

The constraints in the parallel robot design involves: the maximum torque of the actuators (16) which establishes the real torque limits; the mobility of the robot (17) which is stated by the five-bar Grashof criterion; the real limits in the geometric design variables (18); the trajectory specification (19) to be followed by the end-effector of the five-bar parallel robot; and the parallel robot dynamic model (3).

$$
|u_i(t)| \leq u_{i\max} \quad \text{for } i = 1 \text{ to } 2,\ 0 \leq t \leq t_f \tag{16}
$$

$$
\begin{gathered}
a_{s_5} + a_{s_1} + a_{s_2} - a_{s_3} - a_{s_4} < 0 \\
\begin{aligned}
a_{s_1} + a_{s_2} - a_{s_3} < 0 \qquad & a_{s_3} - a_{s_5} < 0 \\
a_{s_1} + a_{s_2} - a_{s_4} < 0 \qquad & a_{s_4} - a_{s_5} < 0 \\
a_{s_5} - a_{s_{\max}} \leq 0 \qquad & -a_{s_1} + a_{s_{\min}} < 0
\end{aligned} \\
-a_{s_2} + a_{s_{\min}} < 0
\end{gathered} \tag{17}
$$

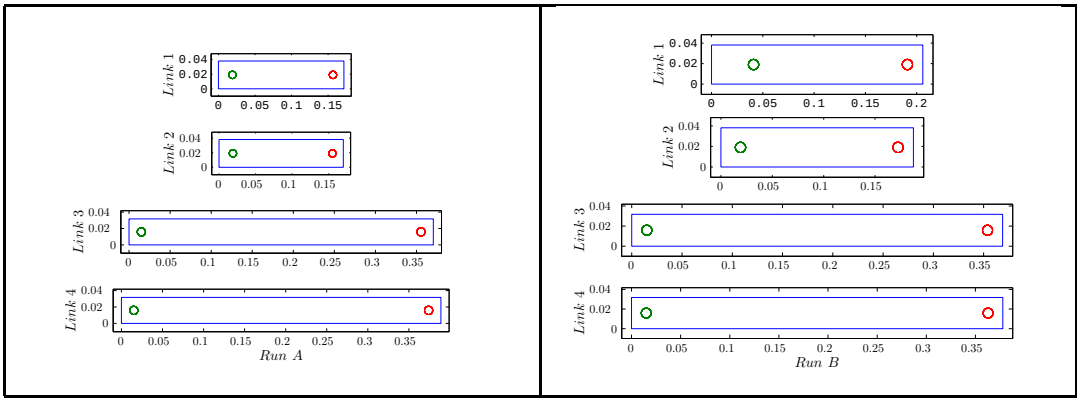

Figure 8. Schematic representation of optimal structures of parallel robot links for runs A and B (units in (m)).

are shown in Table A3. The optimal link shapes have symmetric appearance as they are displayed in Fig. 8.

On the other hand, the optimal dynamic parameter of the links with the optimal geometric parameters found in run A and run B are shown in Table A4 and Table A5, respectively. It is important to remark that the mass center angle γ_i of all links $(i = 1, ..., 4)$ are around zero radians because $f^*_{s_i}$ and $g^*_{s_i}$ tend to zero, and because the geometric parameter $b^*_{s_i}$ satisfies $b^*_{s_i} < a^*_{s_i} + d^*_{s_i}$ (see Fig. 2).

We highlight the following issues with respect to all runs: The design variables $f^*_{s_i}$, $g^*_{s_i}$, $h^*_{s_i}$, $i^*_{s_1}$, $j^*_{s_i}$, $k^*_{s_i}$ for $i = 1$ to 4 may not be taken into account in the optimization process because they do not improve the system performance both circle and Lissajous curve as the desired trajectories. Thus, the convergence required time of the CHDE algorithm could be reduced. For the circle, the design result of run A is better than design results of runs 1-5, because its design provides the best performance function value due to the modified stop criterion. Furthermore, run A renders symmetric link shapes. For the Lissajous curve, link shapes are symmetric too. It is clear that different trajectories (changes in the optimization problem) give different optimum design variables. Nevertheless, the same modified stop criterion could be used for changes in the optimization problem e. g., changes in the desired trajectory. Hence, the modified criterion is very useful for design problems with several design variables because the interruption of the CHDE algorithm is not prematurely done, besides changes in the optimization problem (different desired trajectory) could be considered.

In general, the optimal PID controller for all runs performs adequately. In order to show the PID control performance, the trajectory tracking of the design results of run A and run 5 is shown in Fig. 9. The errors for run A and run 5 are around $1E-04\,\mathrm{m}$ and $1.5E-04\,\mathrm{m}$, respectively. Both design results present a good performance with respect to the trajectory tracking but the best of them is the design result of run A because the end-effector of the design result of run A almost reaches the desired trajectory (see Fig. 9b).

For the Lissajous curve, trajectory tracking with the optimal PID controller of the design results of run B is displayed in Fig. 10. The trajectory tracking error is around $4E-04\,\mathrm{m}$.

On the other hand, singularity configurations for the five-bar parallel robot are carried out when the unactuated angles (q_3 and q_4) have values of 0 or $\pm\pi$ radians. As it can

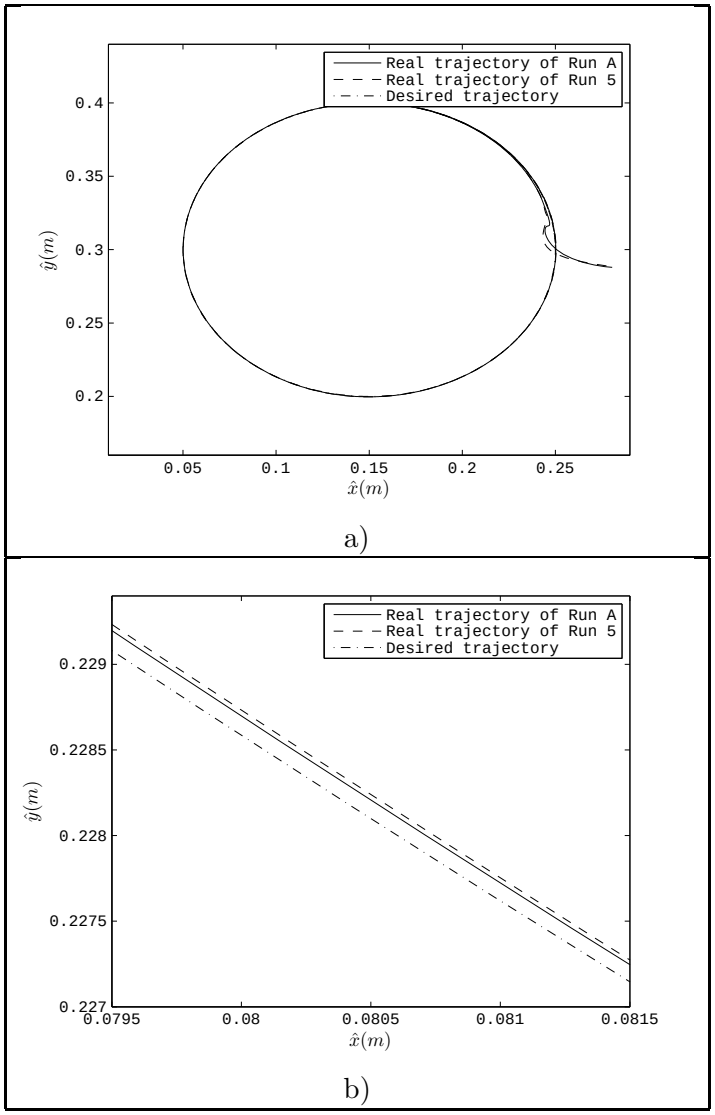

Figure 9. a) Behavior of the end-effector position of the parallel robot with designs of run A and 5. b) Detail of Fig. a).

be seen in Fig. 11, the behavior of the unactuated angles for the trajectory tracking do not reach singularity configurations neither for run A nor for run B. Hence, minimizing the performance function stated in (20), the position error is minimized and singularity configurations of the five-bar parallel robot for the trajectory tracking are avoided.

It is important to note in Fig. 12, that constraints related to real torque limits (5 Nm) are fulfilled.

6. Conclusions and future work

In this paper, a structure-control design of the five-bar parallel robot for trajectory tracking and singularity avoidance is stated. This is formulated as a nonlinear dynamic

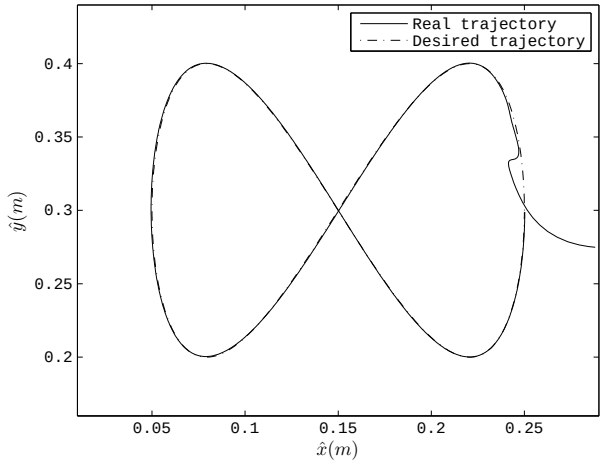

Figure 10. Behavior of the end-effector position of the parallel robot with the design of run B.

optimization problem, where the system dynamics (nonlinear differential equations) is considered as an equality constraint. This problem is solved by a constraint-handling differential evolution algorithm. Two different desired trajectories are chosen.

Fifty one design variables which involve both structure and control aspects are proposed. As the stop criterion influences the convergence of optimization algorithms, different stopping criteria may vary the found optimum results. A good stop criterion for this problem would be that all individuals of the population become similar to each other because some other stop criterion requires a priori knowledge of the problem at hand (e. g. maximum number of generations). In addition, using that criterion, the CHDE algorithm can exhaustively search the optimal results in spite of changes in the design problem e. g. changes in the desired trajectory and in spite of having several design variables.

The CHDE algorithm finds all design variables that improve a dynamic performance function value. The algorithm spends a reasonable time to converge to optimum solutions. In spite of having a large number of design variables and a highly constrained dynamic optimization problem, the CHDE algorithm efficiently works in searching the optimum design variables.

The design results of all runs of the algorithm considering a circle as the desired trajectory are good solutions since all provide similar performance function value. Nevertheless, from a design point of view, the best performance function value is obtained when the modified stop criterion is used (run A), resulting in a design with symmetric link shapes.

Both the geometric parameters and the PID control gains are simultaneously found in one single design step. A synergetic interaction of the structure and the control design is carried out, where the best trade-off between both behaviors is taken into account at the end of the optimization process.

Optimal results show that the mass center angles γ_i of the links, in an interval $(0, \pm\pi]$ radians, do not improve the position error and the singularity avoidance. Only the discrete value of 0 radians in the mass center angles could improve the performance of the five-bar parallel robot.

Future work involves the experimental implementation of the presented approach. On the other hand, one issue in engineering that deserves some further study is the develop-

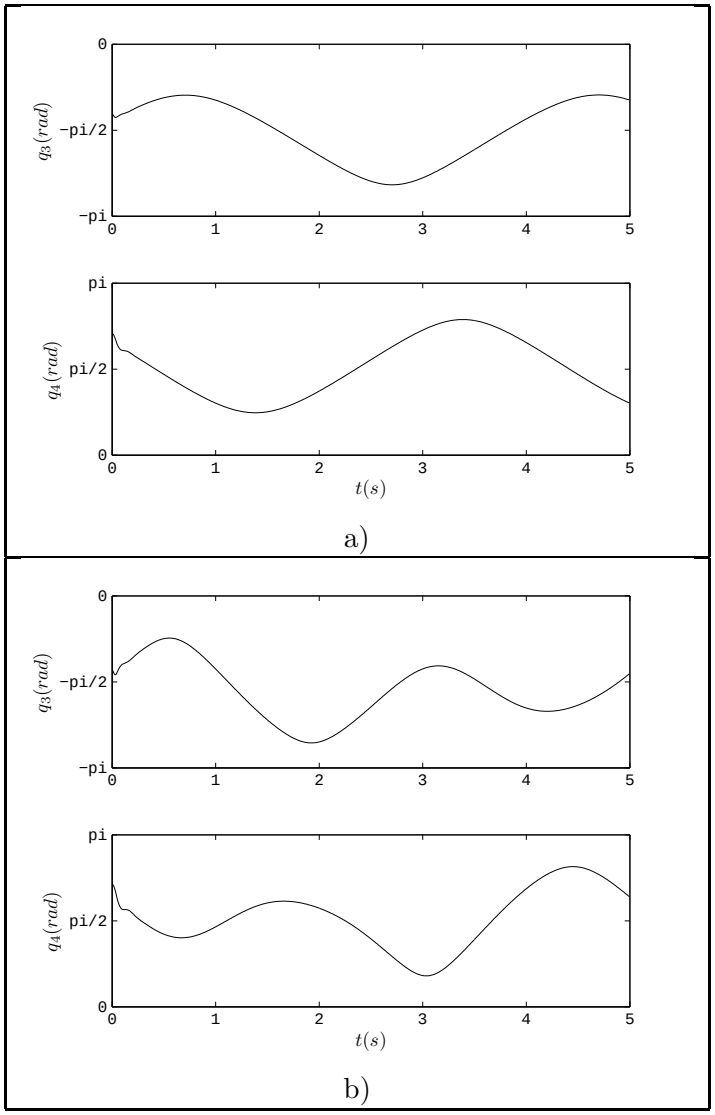

Figure 11. a) Behavior of the unactuated angles. a) Run A (circle) and b) Run B (Lissajous curve).

ment of a robust design not sensitive to variations on the trajectory, since it is important to develop an optimal mechatronic system with an optimal performance for multiple purposes (multiple tasks).

Acknowledgements

The first author acknowledges support from the Mexican Consejo Nacional de Ciencia y Tecnología (CONACyT) through a scholarship to pursue graduate studies at CINVESTAV-IPN, Electrical Engineering Department. All authors acknowledge support from CONACyT, via the project number 084060.
The fourth author acknowledges support from the COFAA and EDI programs of the

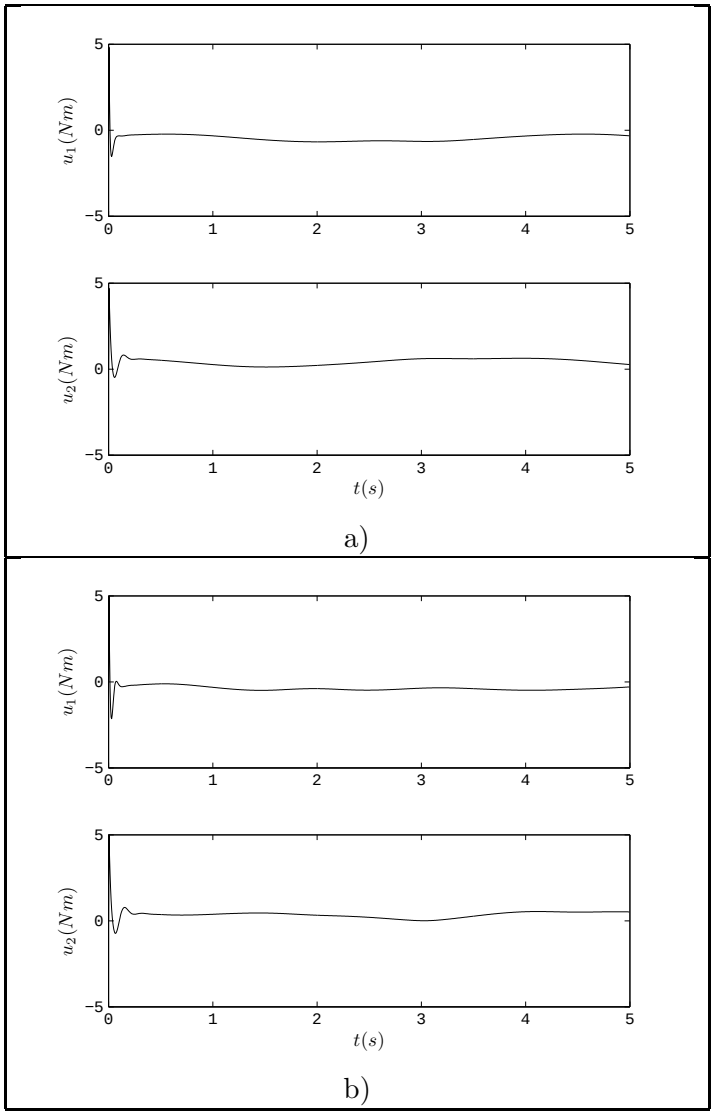

Figure 12. a) Behavior of the control signal. a) Run A (circle) and b) Run B (Lissajous curve).

Instituto Politécnico Nacional and support from SNI-CONACyT.

References

Affi, Z., EL-Kribi, B., and Romdhane, L., 2007. Advanced mechatronic design using a multi-objective genetic algorithm optimization of a motor-driven four-bar system. *Mechatronics*, 17 (9), 489–500.

Alvarez-Gallegos, J., Cruz-Villar, C.A., and Portilla-Flores, E.A., 2005. Vol. 3789 of *Lectures Notes in Artificial Intelligence*, Evolutionary Dynamic Optimization of a Continuously variable Transmission for Mechanical Efficiency Maximization. *In*: *MICAI 2005: Advances in Artificial Intelligence.*, 1093–1102 Springer.

Betts, J.T., 2001. *Practical methods for optimal control using nonlinear programming.*

Society for Industrial Mathematics.

BrysonJr., A.E., 1999. *Dynamic Optimization*. Addison-Wesley Longman Inc.

Cruz-Villar, C.A., Alvarez-Gallegos, J., and Villarreal-Cervantes, M.G., 2009. Concurrent redesign of an underactuated robot manipulator. *Mechatronics*, 19, 178–183.

Deb, K. and Kain, S., 2003. Multi-Speed Gearbox Design Using Multi-Objective Evolutionary Algorithms. *Journal of Mechanical Design*, 125 (3), 609–619.

Ghorbel, F.H., *et al.*, 2000. Modeling and set point control of closed-chain mechanisms: theory and experiment. *IEEE Transactions on Control Systems Technology*, 8 (5), 801–815.

Hibbeler, R.C., 2003. *Engineering mechanics : Statics & dynamics*. Prentice-Hall.

Hunt, K.H., 1983. Structural kinematics of in-parallel-actuated robot-arms. *Journal of Mechanism, Transmissions and Automation in Design*, 105 (4), 705–712.

Kameswaran, S. and Biegler, L.T., 2006. Simultaneous dynamic optimization strategies: Recent advances and chanllenges. *Computers and chemical engineering*, 20, 1560–1575.

Kim, J.Y., 2006. Task based kinematic design of a two DOF manipulator with a parallelogram five-bar link mechanism. *Mechatronics*, 16 (6), 323–329.

Klein, C.A. and Blaho, B.E., 1987. Dexterity measures for the design and control of kinematically redundant manipulators. *International Journal of Robotic Research*, 6 (2), 72–83.

Li, Q., Zhang, W.J., and Chen, L., 2001. Design for control - A concurrent engineering approach for mechatronics systems design. *IEEE/ASME Trans. on Mechatronics*, 6 (2), 161–169.

Liu, X.J., Wang, J., and Pritschow, G., 2006. Kinematics, singularity and workspace of planar 5R symmetrical parallel mechanisms. *Mechanism and Machine Theory*, 41 (2), 145–169.

Lung-Wen, T., 1999. *Robot analysis: The mechanics of serial and parallel manipulators*. John Wiley & Sons.

Mayorga, R.V. and Carrera, J., 2006. A manipulator performance index based on the Jacobian rate of change: A motion planning analysis. *In*: *IEEE International Conference on Robotics and Automation*, May., 4220–4226.

Mezura-Montes, E., Coello-Coello, C.A., and Tun-Morales, E.I., 2004. Lecture Notes in Computer Science, Simple feasibility rules and differential evolution for constrained optimization. *In*: *MICAI 2004: Advances in Artificial Intelligence.*, 707–716 Springer.

Mezura-Montes, E., Velzquez-Reyes, J., and Coello-Coello, C.A., 2006. A comparative study of differential evolution variants for global optimization. *Genetic And Evolutionary Computation Conference*, 485–492.

Osyczka, A., 1984. *Multicriterion optimization in engineering with Fortran Programmes*. Halsted Press.

Ouyang, P.R., Li, Q., and Zhang, W.J., 2003. Integrated design of robotic mechanisms for force balancing and trajectory tracking. *Mechatronics*, 13 (8-9), 887–905.

Portilla-Flores, E.A., *et al.*, 2007. Integration of structure and control using an evolutionary approach: An application to the optimal concurrent design of a CVT. *International Journal for Numerical Methods in Engineering*, 71 (8), 883–890.

Price, K.V., Storn, R.M., and Lampinen, J.A., 2005. *Differential evolution: A practical approach to global optimization*. Springer.

Price, K., 1999. *An Introduction to Differential Evolution*. Mc. Graw Hill.

Runarsson, T. and Yao, X., 2000. Stochastic Ranking for Constrained Evolutionary Optimization. *IEEE Transactions on Evolutionary Computation*, 4 (3), 284–294.

Sadegh, N. and Driessen, B., 1999. Minimum time trayectory optimization and learning.

ASME, Journal of Dynamics Systems, Measurement, and Control, 121, 213–217.

Saravanan, R. and Ramabalan, S., 2008. Evolutionary Minimum Cost Trajectory Planning for Industrial Robots. *J. Intell Robot Syst.*, 52, 45–77.

Shiakolas, P., Koladiya, D., and Kebrle, J., 2005. On the optimum synthesis of six bar linkages using differential evolution and the geometric centroid of precision positions technique. *Mechanism and Machine Theory*, 40 (3), 319–335.

Spong, M.W. and Vidyasagar, M., 2004. *Robot Dynamics and Control*. John Wiley and Sons.

Storn, R.M. and Price, K.V., 1995. Differential evolution - a simple and efficient adaptive shceme for global optimization over continuous spaces. *Technical Report TR-95-012, ICSI*.

Ting, K.L., 1986. Five-bar Grashof criteria. *Journal of Mechanism, Transmissions, and Automation in Design*, 108, 533–537.

Vesterstrom, J. and Thomsen, R., 2004. A comparative study of differential evolution, particle swarm optimization, and evolutionary algorithms on numerical benchmark problems. *Congress on Evolutionary Computation*, 2 (1), 1980–1987.

Yoshikawa, T., 1990. *Foundations of robotics*. The MIT Press.

Youcef-Toumi, K., 1996. Modeling, design, and control integration: A necessary step in mechatronics. *IEEE/ASME Transactions on Mecatronics*, 1 (1), 29–38.

Appendix A. Tables

Table A1. Time required, the optimal value, the performance function evaluation (PFE) and the performance function non-evaluation (PFNE) found by the CHDE algorithm for runs 1-5.

Run	Time required/Hrs.	Optimal value	PFE	PFNE
1	16.1152	−0.917998	170051	30049
2	16.83173	−0.918584	180055	20045
3	17.0285	−0.918801	185559	14541
4	16.2727	−0.917816	174154	25946
5	15.9250	−0.918413	164652	35448
Average	16.4346	−0.918322		

Table A2. Time required, the optimal value, the performance function evaluation (PFE) and the performance function non-evaluation (PFNE) found by the CHDE algorithm with the modified stop criterion. The desired trajectory: *A*) Circle, *B*) Lissajous curve.

Run	Time required/Hrs.	Optimal value	PFE	PFNE
A	106.4124	−0.919942	1028410	33890
B	140.0788	−0.871891	1957146	86006

Table A3. Optimal design parameters p^* for each run. x="this parameter does not care".

	p^*	Run 1	Run 2	Run 3	Run 4	Run 5	Run A	Run B
	$a^*_{s_1}$(m)	0.1351	0.1367	0.1354	0.1356	0.1351	0.1374	0.1499
	$b^*_{s_1}$(m)	0.1049	0.1159	0.0807	0.0606	0.0662	$b_{s_{1_{min}}}$	0.0409
	$c^*_{s_1}$(m)	0.0403	0.0504	0.0454	0.0415	0.0401	$c_{s_{1_{min}}}$	$c_{s_{1_{min}}}$
L	$d^*_{s_1}$(m)	0.0185	0.0190	0.0258	0.0234	0.0256	$d_{s_{1_{min}}}$	$d_{s_{1_{min}}}$
I	$e^*_{s_1}$(m)	0.0081	0.0072	0.0064	0.0063	0.0064	$e_{s_{1_{min}}}$	$e_{s_{1_{min}}}$
N	$f^*_{s_1}$(m)	0.0179	0.0123	0.0121	0.0052	0.0012	10.18E-09	36.60E-10
K	$g^*_{s_1}$(m)	0.0120	0.0131	0.0141	0.0216	0.0208	60.53E-08	28.59E-10
	$h^*_{s_1}$(m)	0.1350	0.0500	0.0261	0.1550	0.0703	x	x
1	$i^*_{s_1}$(m)	0.0746	0.0380	0.1405	0.0205	0.0582	x	x
	$j^*_{s_1}$(m)	0.0578	0.1333	0.1486	0.0298	0.0318	x	x
	$k^*_{s_1}$(m)	0.1483	0.1019	0.0357	0.1267	0.0763	x	x
	$a^*_{s_2}$(m)	0.1327	0.1344	0.1342	0.1329	0.1346	0.1358	0.1532
	$b^*_{s_2}$(m)	0.0670	0.0953	0.0484	0.0901	0.0403	$b_{s_{2_{min}}}$	$b_{s_{2_{min}}}$
	$c^*_{s_2}$(m)	0.0425	0.0442	0.0390	0.0441	0.0439	$c_{s_{2_{min}}}$	$c_{s_{2_{min}}}$
L	$d^*_{s_2}$(m)	0.0172	0.0189	0.0213	0.0190	0.0154	$d_{s_{2_{min}}}$	$d_{s_{2_{min}}}$
I	$e^*_{s_2}$(m)	0.0065	0.0066	0.0067	0.0071	0.0070	$e_{s_{2_{min}}}$	$e_{s_{2_{min}}}$
N	$f^*_{s_2}$(m)	0.0048	0.0032	0.0109	0.0095	0.0052	10.70E-08	76.33E-11
K	$g^*_{s_2}$(m)	0.0170	0.0015	0.0016	0.0011	0.0164	13.93E-08	21.44E-10
	$h^*_{s_2}$(m)	0.0553	0.1898	0.1664	0.0486	0.1443	x	x
2	$i^*_{s_2}$(m)	0.0484	0.0069	0.0166	0.1340	0.0318	x	x
	$j^*_{s_2}$(m)	0.1143	0.0833	0.1516	0.1996	0.1545	x	x
	$k^*_{s_2}$(m)	0.0225	0.0906	0.0110	0.0038	0.0190	x	x
	$a^*_{s_3}$(m)	0.3370	0.3384	0.3387	0.3393	0.3382	0.3404	0.3388
	$b^*_{s_3}$(m)	0.0358	0.0294	0.0272	0.0224	0.0487	$b_{s_{3_{min}}}$	$b_{s_{3_{min}}}$
	$c^*_{s_3}$(m)	0.0320	0.0328	0.0318	0.0328	0.0326	$c_{s_{3_{min}}}$	$c_{s_{3_{min}}}$
L	$d^*_{s_3}$(m)	0.01769	0.0201	0.0215	0.0239	0.0205	$d_{s_{3_{min}}}$	$d_{s_{3_{min}}}$
I	$e^*_{s_3}$(m)	0.0065	0.0066	0.0064	0.0065	0.0064	$e_{s_{3_{min}}}$	$e_{s_{3_{min}}}$
N	$f^*_{s_1}$(m)	0.0006	0.0024	0.0012	0.0017	0.0021	15.23E-09	20.97E-11
K	$g^*_{s_1}$(m)	0.0013	0.0011	0.0007	0.0023	47.72E-05	41.34E-11	39.85E-11
	$h^*_{s_3}$(m)	0.2292	0.1981	0.0231	0.2537	0.3863	x	x
3	$i^*_{s_3}$(m)	0.0847	0.0500	0.3002	0.0365	0.0065	x	x
	$j^*_{s_3}$(m)	0.3405	0.0596	0.3046	0.1773	0.1612	x	x
	$k^*_{s_3}$(m)	0.0399	0.1932	0.0792	0.1363	0.1356	x	x
	$a^*_{s_4}$(m)	0.3665	0.3633	0.3617	0.3712	0.3617	0.3589	0.3478
	$b^*_{s_4}$(m)	0.0200	0.0150	0.0158	0.0304	0.0198	$b_{s_{4_{min}}}$	$b_{s_{4_{min}}}$
	$c^*_{s_4}$(m)	0.0322	0.0320	0.0322	0.0350	0.0325	$c_{s_{4_{min}}}$	$c_{s_{4_{min}}}$
L	$d^*_{s_4}$(m)	0.0171	0.0228	0.0283	0.0200	0.0231	$d_{s_{4_{min}}}$	$d_{s_{4_{min}}}$
I	$e^*_{s_4}$(m)	0.0064	0.0064	0.0063	0.0064	0.0066	$e_{s_{4_{min}}}$	$e_{s_{4_{min}}}$
N	$f^*_{s_1}$(m)	0.0036	0.0018	52.41E-06	0.0019	0.0014	74.39E-10	52.50E-11
K	$g^*_{s_1}$(m)	0.0005	0.0023	0.0017	0.0006	0.0011	78.82E-10	62.67E-12
	$h^*_{s_4}$(m)	0.3280	0.2782	0.1252	0.2250	0.2834	x	x
4	$i^*_{s_4}$(m)	0.0194	0.0789	0.0077	0.1065	0.0360	x	x
	$j^*_{s_4}$(m)	0.0863	0.1748	0.0636	0.2197	0.2212	x	x
	$k^*_{s_4}$(m)	0.0895	0.2004	0.0946	0.0589	0.0515	x	x
5	$a^*_{s_4}$(m)	0.3666	0.3633	0.3618	0.3713	0.3617	0.3589	0.3478
	$k^*_{p_1}$	42.74	38.08	37.75	35.60	39.08	33.96	34.54
	$k^*_{i_1}$	163.73	134.00	150.91	116.89	111.37	93.67	129.64
P	$k^*_{d_1}$	1.05	0.8201	0.7623	0.8925	0.9074	0.6509	0.7520
I	$k^*_{p_2}$	20.73	19.56	19.04	21.84	18.81	18.48	13.50
D	$k^*_{i_2}$	150.04	119.16	134.48	175.64	105.20	115.58	77.83
	$k^*_{d_2}$	0.4687	0.3873	0.4511	0.5058	0.4548	0.3896	0.3493

Table A4. Dynamic parameters of the parallel robot links with optimal geometric design variables of run *A*.

Dynamic parameter	Link $i=1$	Link $i=2$	Link $i=3$	Link $i=4$
$m_i^*(\mathrm{kg})$	0.3191	0.3327	0.2044	0.2114
$l_{c_i}^*(\mathrm{m})$	0.0246	0.0291	0.1728	0.1794
$\gamma_i^*(\mathrm{rad})$	$-214.12E-08$	$-8.18E-08$	$3.60E-08$	$-0.206E-08$
$I_i^*(\mathrm{kg\,m^2})$	$66.15E-05$	$82.06E-05$	$239.02E-05$	$266.23E-05$

Table A5. Dynamic parameters of the parallel robot links with optimal geometric design variables of run *B*.

Dynamic parameter	Link $i=1$	Link $i=2$	Link $i=3$	Link $i=4$
$m_i^*(\mathrm{kg})$	0.3416	0.3441	0.2035	0.2053
$l_{c_i}^*(\mathrm{m})$	0.0256	0.0343	0.1720	0.1739
$\gamma_i^*(\mathrm{rad})$	$-92.70E-11$	$-32.32E-10$	$-47.26E-11$	$70.11E-11$
$I_i^*(\mathrm{kg\,m^2})$	$86.34E-05$	$107.66E-05$	$235.94E-05$	$244.06E-05$